Tracking Control Properties of Human–Robotic Systems Based on Impedance Control

Toshio Tsuji, *Member, IEEE,* and Yoshiyuki Tanaka, *Member, IEEE*

Abstract—Human–robotic systems that include interaction between human operators and robots should be designed with careful consideration for the dynamic property and control ability of a human operator. This paper performs manual tracking control tests on a human–robotic system using an impedance-controlled robot, and investigates control characteristics of a human operator according to the robot impedance properties. Experimental results demonstrate that humans try to maintain dynamic properties of an overall system as constant as possible by adjusting their own impedance properties. Then, a new training system using a neural network for operating a human–robotic system is constructed on the basis of the experimental findings in the human tracking control properties.

Index Terms—Human–robotic systems, impedance control, man–machine systems, neural network (NN), tracking test, training system.

I. INTRODUCTION

DEVELOPMENT of an advanced robot system has been anticipated for tasks such as tending patients and elderly persons in hospitals, assisting a human worker at a general office, and so on [1]–[3]. In such human–robotic systems, a human operator often takes the initiative in executing tasks; in contrast, robots are required to assist the operator's movements. Therefore, such a system should be designed with careful consideration of the control properties of a human operator, as well as the control accuracy and performance of the system, to achieve natural cooperation of a human operator and a robotic device.

Many methods have been proposed for designing and controlling a human–robotic system constructed with an impedance-controlled robot. In such studies, control properties of a human operator are usually expressed with mechanical impedance parameters such as inertia, viscosity, and stiffness. Therefore, the overall system can be described by the impedance property because dynamic behaviors of the robot are modeled by impedance properties. Such systems using an impedance model can be grouped roughly into two types: the first is a power-assist system which executes a task by the amplified human force [4]–[7] ; the second is a human–robotic cooperation system in which robots supplement the human operator with an assistive force [8]–[14]. Also, those previous

studies can be classified into two types according to whether the human impedance property is constant during operation [4]–[6], [8], [9], [13], or variable [7], [10], [11], [14]. No detailed discussion has addressed how human operators adjust their impedance characteristics according to a given task and change control properties during operation.

The human operator can change his/her hand impedance by regulating the arm posture [15], [16] and the muscle-contraction levels [17]–[19] to maintain system stability even if the robot has an unstable impedance [20]. In addition, it has been suggested that the human impedance is affected so much by the operator's proficiency at the task. Consequently, we must investigate dynamic properties and the control ability of human operators according to the control property of a robotic device for designing an effective and safe human–robotic system.

The main purpose of this study is to examine how the tracking control properties of the human–robotic system change according to the robot impedance and the human arm impedance. In this paper, a series of tracking tests are executed by using the developed human–robotic system utilizing an impedance-controlled robot. Experimental results demonstrate that humans attempt to maintain dynamic properties of the overall system as constant as possible by adjusting their own impedance properties.

Experimental findings obtained in this paper may be used as basic data for determining the impedance characteristics of power-assist systems, and also for the structural design of manual control training devices using robots such as prosthetic and orthosis systems for the physically handicapped [21]. Such human–robotic systems are intended to provide effective human support through assisting the limited motor capability of the operator with robotic manipulators. To attain that goal, it is necessary not only to establish the robot-control technology for assisting a human operator, but also to supply an effective training system for improving the operator's control ability.

Several studies have examined such a training system using a neural network (NN) for a human operator [22]–[24]. However, previous training systems may have difficulty in adapting to the individual differences of motor control ability and the proficiency of a trainee in real-time because of their system structures. For those reasons, the present study is attempted to develop an adaptive training system using a NN with consideration of the human control properties. The system uses only one NN to modify control parameters to adapt such individual differences while identifying nonlinear control characteristics of the overall system including a human operator in real-time. Developing an effective training system is another important goal of this study.

The authors are with the Artificial Complex Systems Engineering, Hiroshima University, Hiroshima 739-8527, Japan (e-mail: tsuji@bsys.hiroshima-u.ac.jp; ytanaka@bsys.hiroshima-u.ac.jp).

This paper is organized as follows. Section II describes related work on human–robotic systems and training systems using NNs. Section III explains the structure of a human–robotic system and the experimental method in this study. Section IV investigates human control properties according to the robot impedance and the arm posture of a human operator. Finally, a design method using NN of an adaptive training system is discussed in Section V.

II. RELATED WORKS

A. Human–Robotic Systems

Kazerooni [4] proposed a power-assist system with a single robot, and estimated the human impedance from frequency responses of the system. Yokokohji *et al.* [6] and Colgate [7] studied the human impedance property in manipulation of a teleoperation system. Particularly, Yokokohji *et al.* [6] analyzed system stability using an impedance model of the human operator. Regarding the human–robotic cooperation system, Kosuge *et al.* [8], [9] estimated human impedance from frequency responses using the least squares method. Al-Jarrah *et al.* [10], [11] expressed the dynamic property of the human operator with stiffness and reported that the system stability is much influenced by the stiffness. Ikeura [13] investigated the impedance property of a human operator who manipulated a slave robot to follow the motion of the master robot that was controlled by another operator, and reported that the operability of master-slave systems can be improved by applying the estimated human impedance to the impedance control of the slave robot. Furthermore, Tsumugiwa *et al.* [14] discussed a variable impedance control method of a robot based on human arm stiffness estimated during human–robotic cooperative tasks.

B. Training Systems Using NNs

A basic design method for a training system for operating human–robotic systems is to give technical assistance to a trainee to alleviate the burden during the skill acquisition process. This kind of training is based on the idea that a human easily understands a given control task and the characteristics of a controlled system through appropriate assistance; therefore, the speed of the skill acquisition process would be accelerated.

Several studies have reported training systems for human operators. For example, Kraiss [22] proposed a method to assist a car driver using an NN. The NN used in his method identifies the human characteristics through learning. However, this method may require a large NN and cause difficulty during the learning procedure. Krishnakumar *et al.* [23] developed a helicopter hovering training system. However, it is difficult to evaluate the degree to which a trainee acquires the control ability and realized the desired characteristic because a desired control characteristic is not used as a training target of the task. In addition, Suenaga [24] proposed a manual preview-predictive control system that provides a future reference signal and a predicted value of the control variable to the operator. He showed that the method was effective in compensation for human delay and improvement of the control performance, but the validity of the method is strictly limited because the identified model of human operator's properties is assumed to be linear.
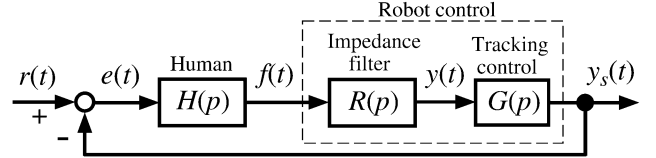
Fig. 1.   Control structure of the human–robotic system.
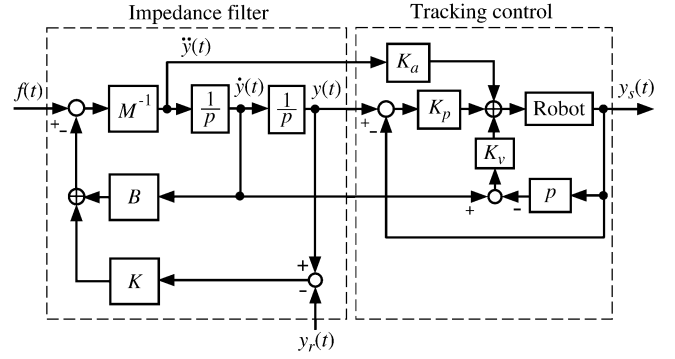
Fig. 2.   Detailed structure of the robot control part.

III. EXPERIMENTAL METHODS

A. Structure of Human–Robotic System

Fig. 1 shows a block diagram of a human–robotic system that is a single-input-single-output (SISO) system [25]. The target task in this system is that an operator is asked to manipulate the impedance-controlled robot with his hand force $f(t)$ and to minimize the control error $e(t)$ between the desired signal $r(t)$ and the robot's position $y_s(t)$ by using the visual-feedback information.

A transfer function of the impedance-controlled robot $R(p)$[26], [27] is given as

$$R(p) = \frac{1}{Mp^2 + Bp + K} \tag{1}$$

where M, B, and K represent the inertia, viscosity, and stiffness of the end-effector, respectively, and p is the differential operator. Then, we presume that the robot's current position $y_s(t)$ almost agrees with the desired position of the impedance control $y(t)$, an output from the impedance filter, in a certain bandwidth of frequency so that $G(p) \approx 1$ is held.

Fig. 2 shows a detailed block diagram of the robot control part, where $y(t)$ is the desired position of the impedance control, $y_r(t)$ the equilibrium point of the robot stiffness. The impedance filter computes the robot's desired position $y(t)$ from the operational force $f(t)$ and the impedance model given by (1). The tracking control block works to minimize the error between $y(t)$ and $y_s(t)$ by adjusting the position feedback gain K_p, the velocity feedback gain K_v, and the acceleration feedforward gain K_a so as to realize $G(p) \approx 1$.

B. Experimental System

Fig. 3 shows an overview of the experimental system, which includes a robot, a computer for robot control, and a visual feedback display to provide the control error $e(= r - y_s)$ for a subject. A linear motor table with one degree of freedom (Nippon Thompson Co., Ltd., encoder resolution: 1.0 [μm], maximum
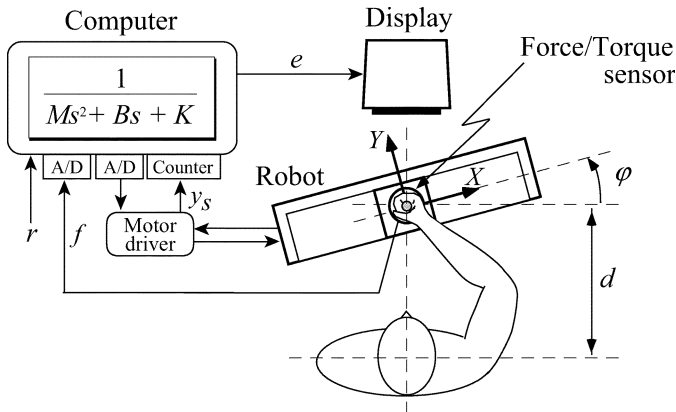
Fig. 3. Experimental apparatus.

power: $\pm 10 \times 9.8$ [N]) is used as a robot in this system. A handle and a six axis force/torque sensor (BL Autotec Co., Ltd., resolution ability: force x axis, y axis: 0.005 [N], z axis: 0.15 [N], torque: 0.003 [Nm]) are attached to the moving part of the robot to measure the hand force f imposed by a human operator. The handle (hand) position is measured by an encoder built into the linear motor table. Then, the operational direction ψ can be changed by means of the rotary motor set under the table.

Fig. 4 illustrates the detailed experimental apparatus to carry out the target task. A human subject can operate the handle attached at the linear motor table with one degree-of-freedom, while the control error e is shown with the position of the circle on the visual feedback display. In the experiments, a subject is asked to follow the reference signal r via positioning the circle at the desired point, at which the control error e becomes zero, with the visual feedback information. Therefore, when a subject can completely follow the reference signal, the circle always locates at the desired point on the display.

A target signal r used in this paper is a kind of random signals generated from white noise filtered by a second order Butterworth filter (cut-off frequency: 0.5 [Hz]) with maximum amplitude 0.1 [m], so it changes relatively slowly but a human subject cannot predict how the target signal changes in the future. The equilibrium point of the robot stiffness y_r was set at the origin of the operational task space that is located at distance $d = 0.55$ [m] in front on the centerline of the body (see Fig. 3).

The robot was controlled with the sampling rate of 1 [kHz], and the characteristics of the system were analyzed by using the measured data with the sampling rate of 25 [Hz].

IV. TRACKING CONTROL EXPERIMENTS

A. Experimental Procedure

Four male subjects (graduate students of average height and weight: aged 22–24) conducted tracking experiments. They had never taken part in the tracking test using the constructed system.

Two types of experiments were designed to investigate tracking control properties of a human operator:

Task 1. Control with movable-handle: A subject carries out tasks where the robot's handle can be moved with his hand force.

Task 2. Control with fixed-handle: A subject carries out tasks where the robot's handle is fixed at the origin of the operational task.

Note that it is difficult for a human operator to regulate dynamic properties of his/her hand movements in view of the human impedance model when the robot handle is fixed, because he/she cannot change the arm posture as he/she needs.

Each type of experiments was conducted with the five different natural frequencies $\omega_n = \sqrt{(K/M)} = 2, 4, 6, 8, 10$ [rad/s] under $K = 55$ [N/m] and $\zeta = 1$; the eight different damping coefficients $\zeta = (B/(2\sqrt{MK})) = 0, 0.5, 1, 1.5, 2, 2.5, 3, -0.5$ under $K = 55$ [N/m] and $\omega_n = 4$ [rad/s]; and the eight different stiffnesses of the robot $K = 0, 27.5, 55, 82.5, 110, 137.5, -27.5, -55$ [N/m] under $M = 3.43$ [kg] and $\zeta = 0$. Subjects were first asked to execute tasks under the stable conditions ($\xi \geq 0$; $K \geq 0$), and then under the unstable condition ($K = -27.5, -55$ [N/m]; $\zeta = -0.5$). The experimental time per trial was 60 [s], and a set of experiments was done with a two or three minute intermission between trials.

Fig. 5 shows an example of the time histories of the target signal r, the hand position y_s, the control error e, the hand force to the motion direction f_x, and the hand force to the normal direction f_y under $\varphi = 0$ [rad], $\omega_n = 6$ [rad/s], $\zeta = -0.5$, and $K = 55$ [N/m]. Note that the subject operated the unstable robot with $\zeta = -0.5$ after he had carried out all tests under the stable conditions. It can be seen that the subject actively controls the tangential force f_x according to the control error.

To quantitatively evaluate proficiency in the target task, the following performance indexes J and U_x are defined:

$$J = \frac{\int_0^{t_f} e^2(t)dt}{\int_0^{t_f} r^2(t)dt} \tag{2}$$

$$U_x = \frac{\int_0^{t_f} f_x^2(t)dt}{\int_0^{t_f} r^2(t)dt} \tag{3}$$

where J is the normalized square sum of positional errors, and U_x is the normalized square sum of hand force in the operational direction f_x (see Fig. 3). It is expected that both J and U_x will decrease as the subject attains proficiency.

Fig. 6 shows an example of the changes of J and U_x with respect to the number of trials under $\omega_n = 6$ [rad/s], $\zeta = -0.5$, and $K = 55$ [N/m]. The successive trials are connected by a solid line. J is almost larger than 1 and U_x changes greatly during the first 30 trials. Subsequently, J is less than 1 and U_x retains smaller values. These results show that the human operator can gradually acquire tracking ability through repeated operation, even in inexperienced conditions.

The present paper analyzes dynamic properties of a human operator during the last ten trials after the control performance J reached a steady state (see Fig. 6), where he may have enough ability in the manual tracking control task.
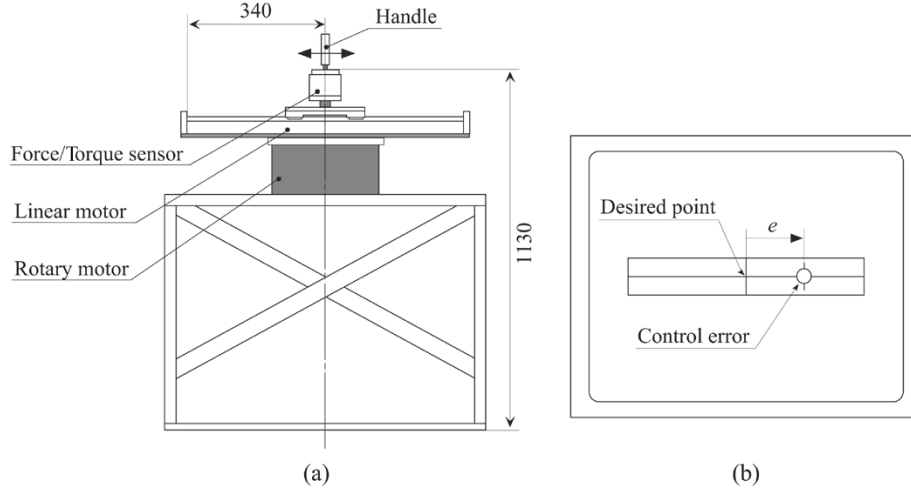
Fig. 4. Detailed structure of the robot part and a screen layout of the visual feedback display.
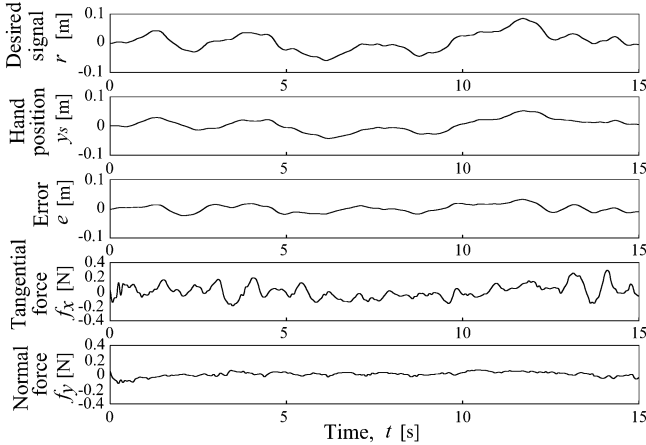
Fig. 5. Example of experimental results for an unstable robot impedance ($K = 55$ [N/m], $\omega_n = 6$ [rad/s], $\zeta = -0.5$, subject A), using the movable handle.

Fig. 6. Change of the control performance J and the normalized square sum of hand force U_x depending on the number of trial ($K = 55$ [N/m], $\omega_n = 6$ [rad/s], $\zeta = -0.5$, subject B), using the movable handle.

B. Human Control Properties According to Robot Impedance With Movable Handle

Fig. 7 shows the changes of the control performance indexes J and U_x using the movable handle, where panels (a)–(c) show the averages and the standard deviations of ten successive trials by the four subjects after the control performance J reached a steady state, depending on the natural frequency ω_n, the damping coefficient ζ, and the stiffness of robot K. Table I represents the average values of J and U_x for all subjects presented in Fig. 7. Note that the total number of trials was different for each human subject because the subjects practiced the specified tracking task until both J and U_x reached a steady state.

Fig. 7(a) shows that both J and U_x increase as ω_n decreases but there exist some differences among subjects. A large force is required for the operation as ω_n decreases, since the inertia M and the viscosity B increase under the conditions in which $\xi = 1$ and $K = 55$ [N/m]. Fig. 7(b) shows that J increases slightly with the increase of ζ while U_x increases so much with the increase of B in which a large force is required for the operation. It should be noted that J and U_x around $\zeta = 1.0$ are better than other conditions in all subjects. Although J increases

TABLE I
MEAN VALUES OF J AND U_x FOR ALL SUBJECTS WITH THE MOVABLE HANDLE

ω_n [rad/s]	2	4	6	8	10			
J	0.62	0.56	0.54	0.53	0.52			
U_x	5.59	1.02	0.46	0.32	0.28			
ξ	-0.5	0.0	0.5	1.0	1.5	2.0	2.5	3.0
J	0.72	0.63	0.60	0.56	0.58	0.59	0.62	0.63
U_x	0.84	0.28	0.45	0.87	1.35	1.73	2.19	2.75
K [N/m]	-54	-27	0	27	54	82	109	137
J	0.67	0.64	0.63	0.61	0.62	0.59	0.60	0.60
U_x	0.92	0.59	0.38	0.30	0.23	0.37	0.44	0.67

when ζ is negative, the subjects follow the target signal by stabilizing the unstable robot; thereby, J falls in around 0.7–0.8. Fig. 7(c) shows that U_x increases so much as K increases because a greater force is needed to operate the robot. It can be seen that both U_x and J increase when K is negative, because

(a) Natural frequency, ω_n (b) Damping coefficient, ζ (c) Robot stiffness, K
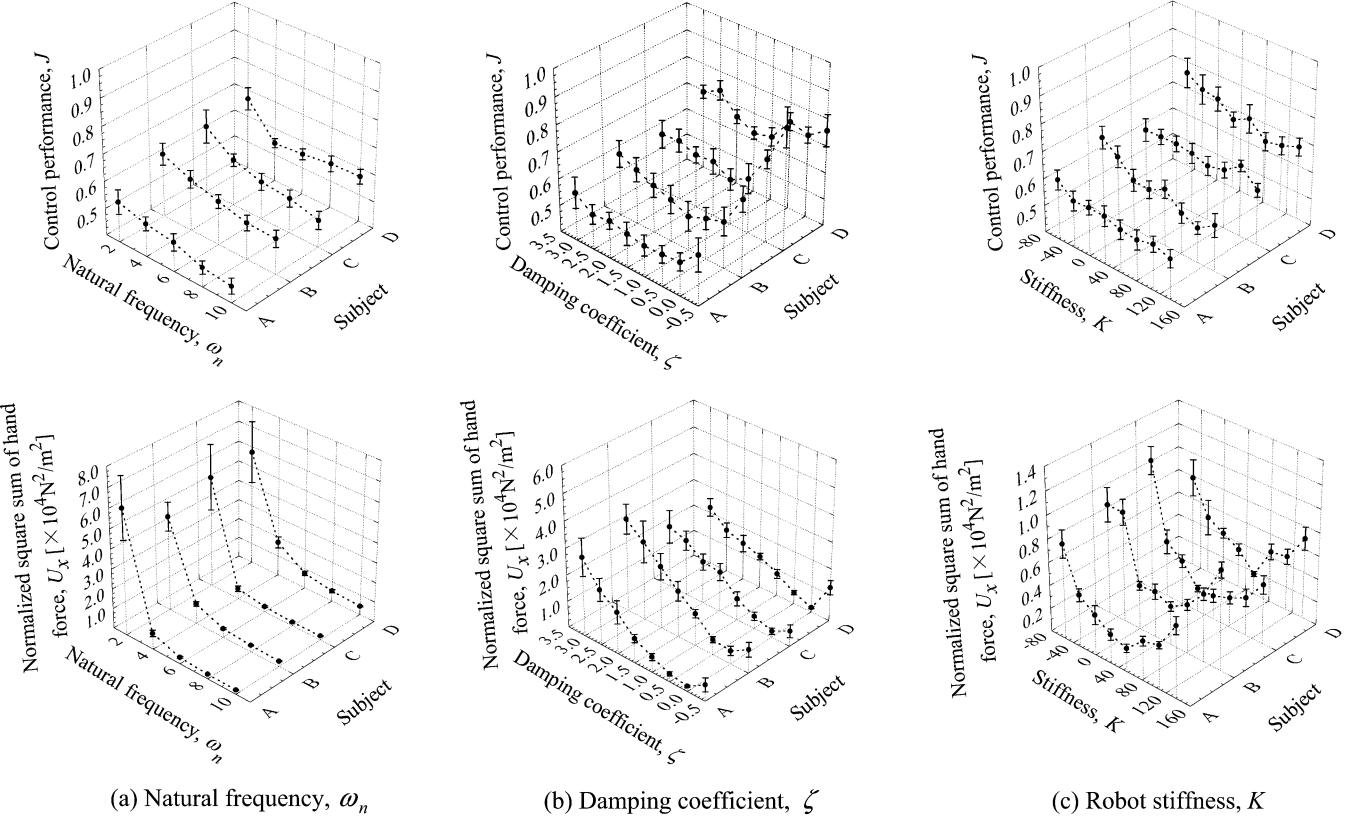
Fig. 7. Change of the control performance J and U_x depending on the natural frequency ω_n ($K = 55$ [N/m], $\zeta = 1$), the damping coefficient ζ ($K = 55$ [N/m], $\omega_n = 4$ [rad/s]), the robot stiffness K ($M = 3.43$ [kg], $\zeta = 0$), using the movable handle. Mean values and standard deviation of 10 trials for each subject are shown.
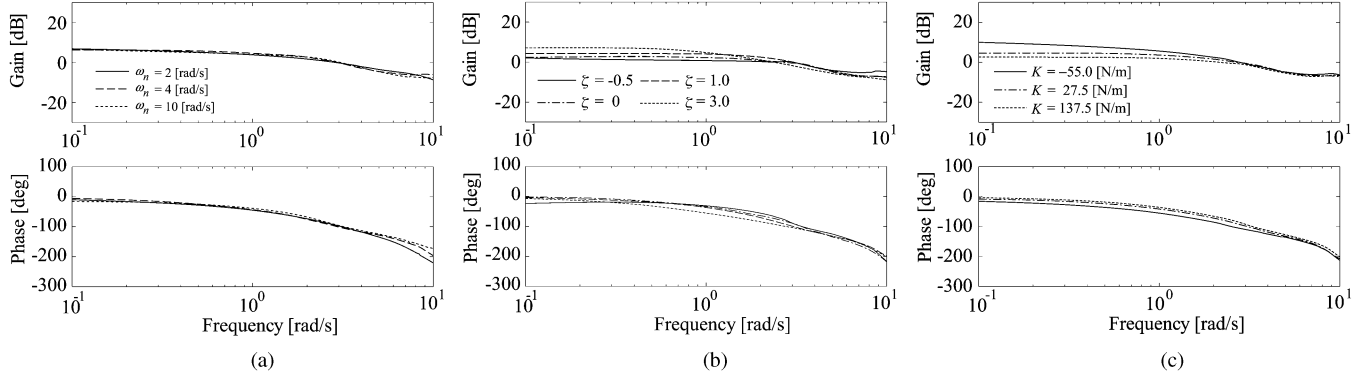
Fig. 8. Estimated describing functions of the human–robotic system $G(j\omega)$ for subject A, using the movable handle.

the operator must handle the unstable robot. All subjects can manipulate the unstable system, and they follow the target signal very well within $K = 0\text{–}137.5$ [N/m].

Descriptive functions of the human–robotic system were estimated from the input and output signals measured during the experiments in the first approximation, although the impedance property of the human arm changes according to the hand position [16]–[20]. The open-loop descriptive function $G(j\omega)$ and the human descriptive function $H(j\omega)$ were identified by the subspace method (N4SID: SubSpace-based State Space model IDentification method) [28], where the input and output signals of $G(j\omega)$ are the control error e and the robot position y_s, while the input and output signals of $H(j\omega)$ are e and the hand force f_x, respectively (See Fig. 2).

Figs. 8 and 9 show examples of the bode diagrams of $G(j\omega)$ and $H(j\omega)$ for Subject A, respectively, according to the natural frequency $\omega_n(= 2, 4, 10$ [rad/s]), the damping coefficient $\zeta(= -0.5, 0, 1.0, 3.0)$, and the robot stiffness $K(= -55.0, 27.5, 137.5$ [N/m]). Each panel represents the average results of ten trials. It can be seen from Fig. 8 that the estimated gain characteristics of $G(j\omega)$ are almost constant regardless of the changes in ω_n, ζ, and K.

On the other hand, the estimated gain characteristics of $H(j\omega)$ change greatly according to the experimental condition. Fig. 9(a) shows that the human operator gain increases in the high frequency range with the reduction of the natural frequency ω_n. This indicates that the human subject increases the natural frequency of his hand movements to compensate
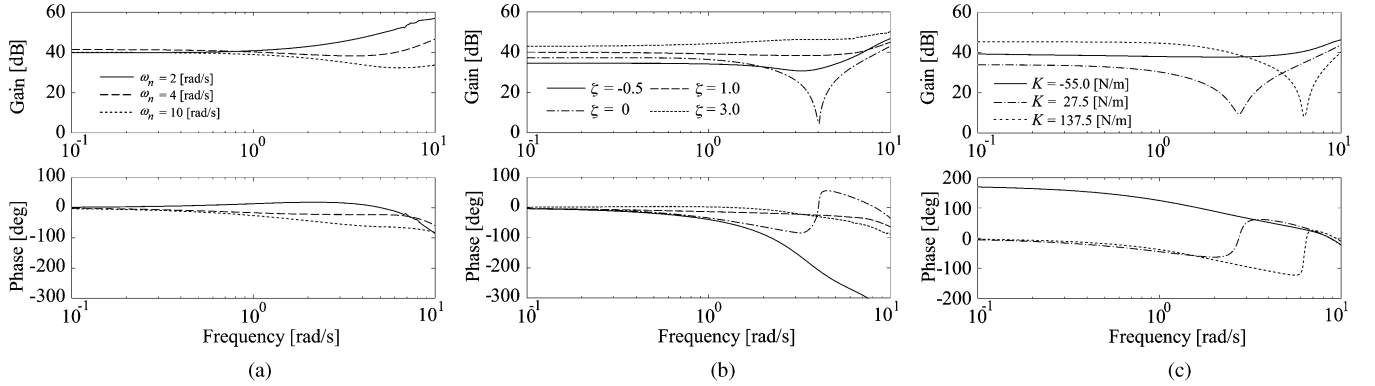
Fig. 9.   Estimated describing functions of the human operator $H(j\omega)$ for subject A using the movable handle.
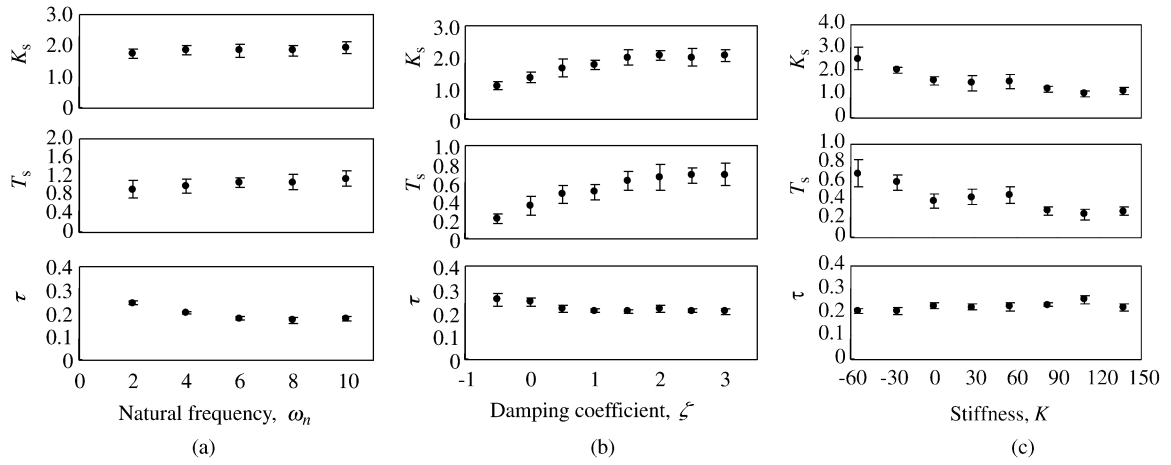
Fig. 10.   Estimated parameters of the transfer function model for the human–robotic system.

for the reduction of natural frequency in the robot impedance, enabling him to cope with rapid changes in the reference signal. Fig. 9(b) shows that the human operator gain changes remarkably according to ξ. Since the frequency characteristics of the robot impedance change considerably depending on ξ, the subject attempts to adapt his control property to keep $G(j\omega)$ constant. On the other hand, in the case of $\zeta = -0.5$, the subject decreases his control gain and greatly changes the phase characteristics in the high frequency range to keep the dynamic properties of the overall system stable including the unstable robot impedance. This indicates that it is possible for human operators to adjust dynamic properties of the overall system even if the robot is unstable, although the value of J increased in the case with $\zeta = -0.5$ as shown in Fig. 7(b). Fig. 9(c) shows that the subject actively regulates his characteristics with respect to K so that the control properties of the overall system can be held almost constant [see Fig. 8(c)], even if the robot stiffness is negative or very large.

These results demonstrate that a human operator adjusts his control properties according to the robot impedance in order to maintain the dynamic properties of the overall system. Generally, in human–machine systems, human operators attempt to maintain the control properties of the overall system by adjusting their own control properties, even if the dynamic properties of the controlled system change [29]. A similar adaptation in human operators can be observed with the con-

structed human–robotic system under the natural frequency $\omega_n = 2$–10 [rad/s], the damping coefficient $\zeta = 0.0$–3.0, and the robot stiffness $K = -55.0$–137.5 [N/m].

Next, control properties of the human–robotic system are modeled using the open-loop descriptive functions $G(j\omega)$, estimated using N4SID [28], with the following transfer function $\tilde{G}(s)$:

$$\tilde{G}(s) = \frac{K_s}{1 + T_s s} e^{-\tau s} \tag{4}$$

where K_s is the gain parameter, T_s is the time constant, and τ is the dead time. These parameters were determined through fitting a bode diagram of $G(j\omega)$, as shown in Figs. 8 and 9, in the transfer function $\tilde{G}(s)$ by the least squares method.

Fig. 10 shows the average and the standard deviations of K_s, T_s, and τ of ten trials depending on the natural frequency ω_n, the damping coefficient ζ and the robot stiffness K. The estimated parameters of $\tilde{G}(s)$ are almost constant under the damping coefficient $\zeta \geq 1$ and $K \geq 0$. It suggests that a human operator tried to maintain the dynamic properties of the overall system by regulating his own control property so as to compensate for the changes of the robot impedance.

On the other hand, the human transfer characteristic $\tilde{H}(s)$ can be approximated from $R(s)$ in (1) and $\tilde{G}(s)$ in (6) by

$$\tilde{H}(s) = \frac{\tilde{G}(s)}{R(s)} = \frac{K_s(Ms^2 + Bs + K)}{1 + T_s s} e^{-\tau s}. \tag{5}$$
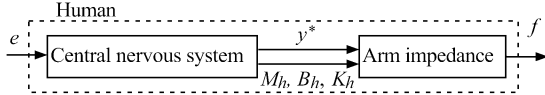
Fig. 11. Human operator model.

Then, a human operator model can be explained as a block diagram illustrated in Fig. 11, which consists of a central nervous system (CNS) and a human arm impedance. The CNS outputs the equilibrium point y^* of the hand stiffness and the desired impedance of the human arm M_h, B_h, and K_h, whereas the other generates the corresponding hand force. The phase lead element in the numerator of (5) is realized by the human arm impedance because the human arm impedance is a second order system, whereas the first-order phase lag element and the time delay element are realized by the CNS. Thus, it can be supposed that the regulation mechanism of human arm impedance has an important role in operating the impedance-controlled robot, which is a second order system, to maintain frequency characteristics of the overall system in the manual tracking control task.

C. Human Control Properties According to Human Arm Impedance With Fixed Handle

The second experiments are performed with the fixed robot handle, where a human subject cannot change the arm posture to regulate the hand impedance properties, even if the subject applies hand force to the robot. Subjects were asked to minimize the error e, as possible, between the virtual robotic position y_s and the target signal r shown on the display. y_s is calculated from the dynamics of the impedance-controlled robot given in (1) with the measured hand force f_x. This experimental condition corresponds to a situation in which the human operator undertakes tracking control with an ordinary human–machine system [29].

Fig. 12 shows changes of the performance indexes J and U_x when the robot handle was fixed, where panels (a)-(c) show the averages and the standard deviations of ten successive trials by the four subjects depending on the natural frequency ω_n, the damping coefficient ζ, and the stiffness of robot K. Note that the data after the control performance J reached a steady state were used. Table II represents the average values of J and U_x for all subjects presented in Fig. 12. The hyphen indicates that the subjects could not control the robotic system during tasks. The experimental conditions and the subjects are the same as those in the first experiments.

The control performance J when the handle was fixed increases remarkably in comparison with the results using the movable handle. On the contrary, the control performance U_x decreases remarkably when the handle was fixed. This indicates that the subjects could not increase their control gain to follow the target signal when the robot handle was fixed. Of greater importance, the robot could not be controlled under the condition in which the damping coefficient was set at $\zeta = -0.5$ [see Fig. 12(b)]. Although the robotic system remains stable under $\zeta = 0$, the subjects hardly follow the target signal because J is much larger than ones in the other conditions. In all cases,

the control performance of the proposed human–robotic system in which the robot handle can be moved, surpasses an ordinary human–machine system in which the robot handle is fixed [29].

Fig. 13 shows changes in the dynamic properties of the overall system $G(j\omega)$ according to the natural frequency ω_n, the damping coefficient ζ and the robot stiffness K, which corresponds to the results in Fig. 8. Compared with the results when the robot handle can be moved, the gain characteristics of the overall system were changed according to the robot impedance properties as shown in Fig. 13. These results indicate that the human operator could not control the overall system as he desired. In the case with $\zeta = 0$, the gain of the overall system considerably decreases compared to the other conditions, and the performance index J remarkably increases (see Fig. 12). Therefore, it was difficult for the subjects to operate the robot while minimizing the control error during the fixed-handle experiments.

These results arise from influences of the human arm impedance on the control property of the overall system. A human can unconsciously regulate the hand impedance in arm movements [15]–[18]. Therefore, in experiments in which the arm is allowed to move concomitant with the robot handle, the subject can regulate impedance properties of the overall system by regulating his own arm impedance. On the contrary, when the handle is fixed, the arm impedance does not affect the impedance characteristics of the overall system. Thus, the control characteristics of the overall system are affected not only by the robot impedance but also by the human arm impedance. This point represents a major difference between the human–robotic system and the ordinary human–machine system [29].

V. NEURO-BASED ADAPTIVE TRAINING SYSTEM OF TRACKING CONTROL

The experimental results discussed in the previous section reveal that a human regulates his/her own impedance properties according to the robot impedance to maintain the dynamic properties of the human–robotic system. Those experimental results may be useful in the design of impedance characteristics in a power assist robot [30] and the composition problem of manual control training with robots [31]. However, in the application of such experimental results into a real human–robotic system, many problems, such as modeling errors, individual differences among human operators, and so on, may occur. To deal with problems such as these, this section aims to propose a novel design method using NN for constructing such human–robotic systems on the basis of the experimental findings, and develops an adaptive training system using NN to discuss the validity of the proposed method.

A. Formulation

A human–robotic system is addressed as a discrete time system because the system is constructed with a digital computer. From Fig. 1 under $G(p) = 1$, the kth output signal of the impedance filter with a sampling interval Δ_t is given as

$$y(k) = R(z^{-1})H(z^{-1})e(k) \qquad (6)$$

(a) Natural frequency, ω_n (b) Damping coefficient, ζ (c) Robot stiffness, K
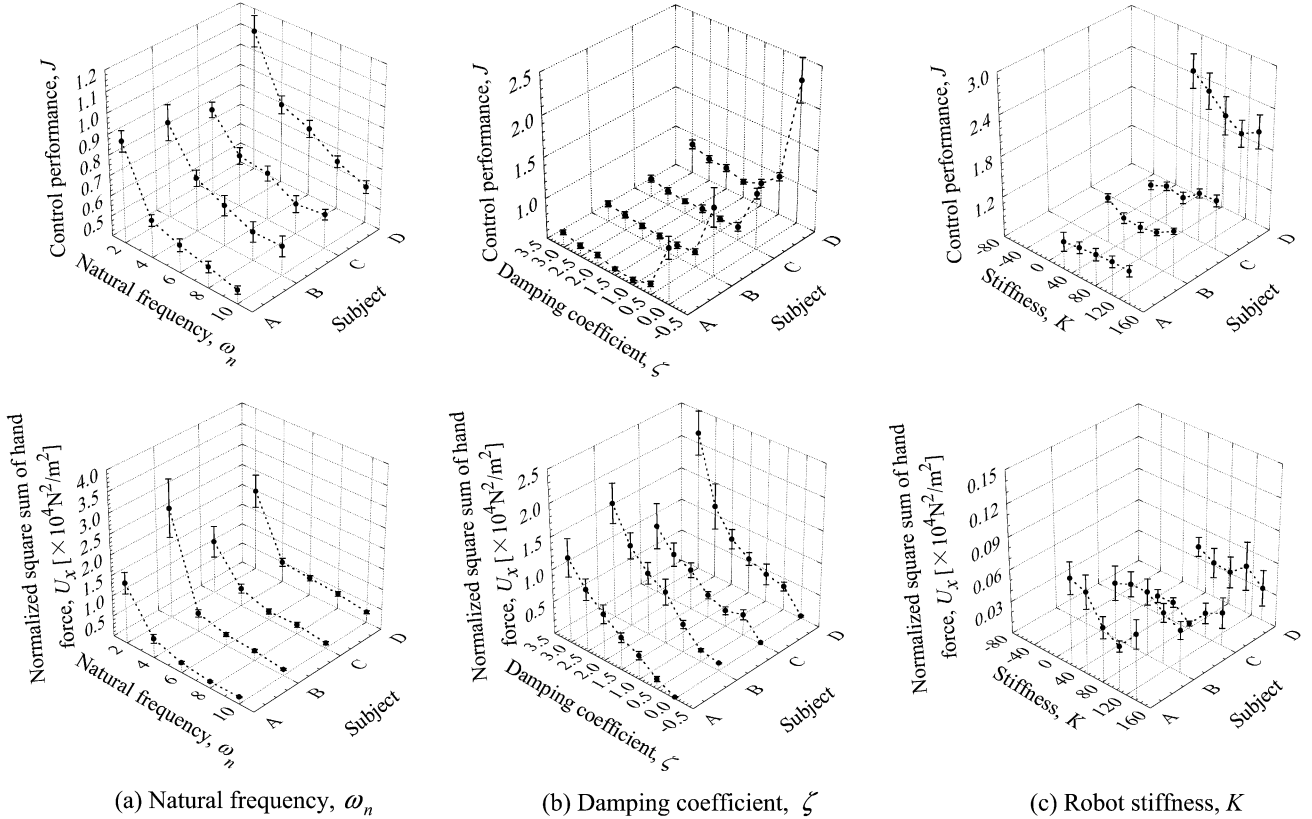
Fig. 12. Change of the control performance J and U_x depending on the natural frequency ω_n ($K = 55$ [N/m], $\zeta = 1$), the damping coefficient ζ ($K = 55$ [N/m], $\omega_n = 4$ [rad/s]), the robot stiffness K ($M = 3.43$ [kg], $\zeta = 0$), in which the handle was fixed. Mean values and standard deviation of ten trials for each subject are shown.

TABLE II
MEAN VALUES OF J AND U_x FOR ALL SUBJECTS
WHERE THE HANDLE WAS FIXED

ω_n [rad/s]	2	4	6	8	10			
J	0.92	0.67	0.63	0.56	0.54			
U_x	1.86	0.46	0.29	0.25	0.18			
ξ	-0.5	0.0	0.5	1.0	1.5	2.0	2.5	3.0
J	–	1.49	0.74	0.66	0.65	0.68	0.70	0.75
U_x	–	0.05	0.26	0.37	0.55	0.76	1.02	1.57
K [N/m]	-54	-27	0	27	54	82	109	137
J	–	–	–	1.45	1.39	1.32	1.34	1.42
U_x	–	–	–	0.05	0.05	0.04	0.04	0.04

where $H(z^{-1})$ and $R(z^{-1})$ denote the dynamic characteristics of a human operator and the ones of the impedance filter, respectively. The term $R(z^{-1})H(z^{-1})$ is expressed as

$$R(z^{-1})H(z^{-1}) = [1 + \Delta_{\mathrm{RH}}(z^{-1})]R_n(z^{-1})H_n(z^{-1}) \quad (7)$$

including an unknown multiplicative modeling error $\Delta_{\mathrm{RH}}(z^{-1})$[32], where $R_n(z^{-1})H_n(z^{-1})$ is the reference model: the target training property of the overall system.

On the other hand, an open-loop transfer function with robotic assistance is defined as

$$R_s(z^{-1})H_s(z^{-1}) = [1 - \Delta_s(z^{-1})]R(z^{-1})H(z^{-1}) \quad (8)$$

where $\Delta_s(z^{-1})$ is a controller for robotic assistance. Therefore, if the target property $R_n(z^{-1})H_n(z^{-1})$ is equivalent to (8), the system output with the robotic assistance agrees with that of the target property. From (7) and (8), the following relationship can be derived as

$$\Delta_s(z^{-1}) = \frac{\Delta_{\mathrm{RH}}(z^{-1})}{1 + \Delta_{\mathrm{RH}}(z^{-1})}. \quad (9)$$

However, the modeling error $\Delta_{\mathrm{RH}}(z^{-1})$ is unknown. For that reason, it is impossible to directly obtain the controller for assistance $\Delta_s(z^{-1})$. Therefore, to overcome this problem on $\Delta_s(z^{-1})$, we introduce an NN into the training system.

B. Structure of Proposed Training System

Fig. 14 shows a block diagram of the proposed training system. The identification model consists of the reference model $R_n(z^{-1})H_n(z^{-1})$ and the NN. The output of the identification model $\hat{y}(k)$ is the sum of the NN's output $y_{\mathrm{NN}}(k)$ and the reference model's output $y_n(k)$. The teacher signal of the NN in the proposed system is the output signal $\hat{y}(k)$ from the reference model of the overall system $R_n(z^{-1})H_n(z^{-1})$ where the input signal is the control error e.

The assisting signal Δ_y is defined using $y_{\mathrm{NN}}(k)$ as

$$\Delta_y(k) = \alpha y_{\mathrm{NN}}(k) \quad (10)$$

where α ($0 \leq \alpha \leq 1$) is the assist ratio. By changing α, the amount of robotic assistance can be adjusted for a trainee. Under $\alpha = 1$, characteristics of the training system concur with those
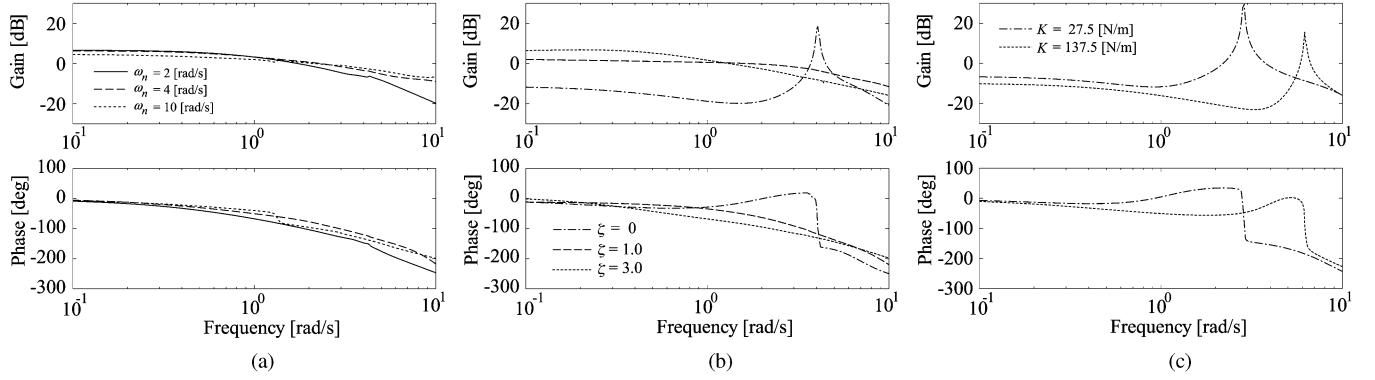
Fig. 13. Estimated describing functions of the human–robotic system $G(j\omega)$, in which the handle was fixed. (a) Natural frequency ω_n (b) the damping coefficient ζ (c) Robot stiffness K.
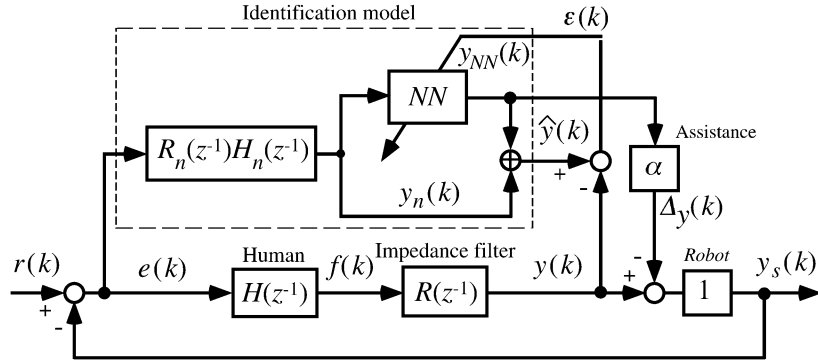
Fig. 14. Block diagram of the proposed training system.

of the reference model $R_n(z^{-1})H_n(z^{-1})$, as explained below. Effective training for a trainee can be realized by adjusting the assist ratio α according to the trainee's control ability.

Here, we analyze the dynamic behavior of this control system. Using (6) and (7), $y(k)$ is expressed as

$$y(k) = y_n(k) + \Delta_{yn}(k) \qquad (11)$$

where

$$y_n(k) = R_n(z^{-1})H_n(z^{-1})e(k) \qquad (12)$$
$$\Delta_{yn}(k) = \Delta_{RH}(z^{-1})y_n(k). \qquad (13)$$

Furthermore, from (8), $y_s(k)$ is represented as

$$y_s(k) = R_s(z^{-1})H_s(z^{-1})e(k) \qquad (14)$$
$$= y(k) - \Delta_y(k) \qquad (15)$$

where

$$\Delta_y(k) = \Delta_s(z^{-1})y(k). \qquad (16)$$

Therefore, with (6), (7), and (12), the assisting signal $\Delta_y(k)$ is obtained by

$$\Delta_y(k) = \Delta_s(z^{-1})[1 + \Delta_{RH}(z^{-1})]y_n(k). \qquad (17)$$

Moreover, the following equation is derived from (17), (9), and (13) as

$$\Delta_y(k) = \Delta_{yn}(k). \qquad (18)$$

On the other hand, $\epsilon(k)$ can be calculated with Fig. 14 and (11) as

$$\epsilon(k) = \hat{y}(k) - y(k) = y_{NN}(k) - \Delta_{yn}(k). \qquad (19)$$

If the NN is well trained, we can expect that the identified error $\epsilon(t)$ becomes zero in (19). Consequently, from (18) and (19), we have

$$\Delta_y(k) = y_{NN}(k). \qquad (20)$$

This reduces to (10) at the assist ratio $\alpha = 1$. In other words, the assisting signal Δ_y can be determined by the output signal of the NN.

Consequently, the proposed method can control a human–robotic system with a modeling error according to characteristics of the given reference model if the NN learns to make the identified error $\epsilon(t)$ in (19) zero in real time. It is notable that the proposed method identifies the control property including characteristics of the human operator. We specifically addressed the overall dynamic property of the human–robotic system that becomes almost constant, but the dynamic property of a human changes greatly depending on the robot impedance property as shown in Figs. 8 and 9. To implement the proposed training system, the reference model as the target property of the training must be determined.

C. Training Experiments

1) Experimental Conditions: The validity of the proposed training system for the manual tracking control task was
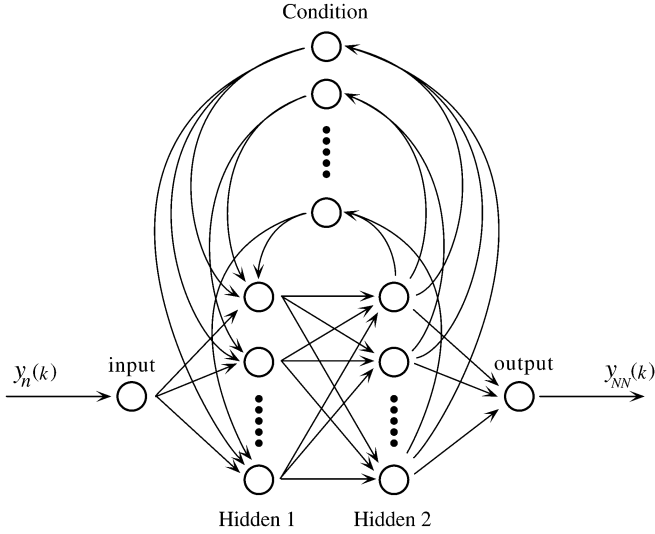
Fig. 15.   Elman network used in the proposed system.

Fig. 16.   Examples of experimental results under the proposed method ($\alpha = 1$, a novice operator).

demonstrated through training experiments by three male subjects (graduate students of average height and weight: aged 22–23) who were not the subjects in Section III and had never operated the experimental system.

The training condition was set as the damping coefficient $\zeta = 1.0$ with $\omega_n = 4$ [rad/s] and $K = 55$ [N/m], in which the performance index J has the minimum value when a human operator has enough ability in the manual tracking control task as shown in Fig. 7(b). After an explanation of the experimental system, the subjects conducted the manual tracking control task without preparation, in which the robot handle can be moved.

The system utilizes the Elman NN [33] with a five-layered structure including an input layer, two hidden layers, an output layer, and a condition layer (see Fig. 15): The number of units in the input layer is 1, 15 in each of the two hidden layers, one in the output layer. The second hidden layer has a recurrent combination with the condition layer that has 15 units. An initial value of the weight ω_{ij} is given using a uniform random number under $|\omega_{ij}| < 0.01$, and the NN learning rate is set at 0.1. In addition, the sigmoid function is used for units in the hidden and the condition layers, whereas the identity function is used for units in the input and the output layers. Online learning is realized by minimizing the identification error $\epsilon(k) = \hat{y}(k) - y(k)$ using the back-propagation algorithm [34] under the condition that the weight in the NN can be updated within the time period of one sampling for the robot control (1.0×10^{-3} [s]).

To avoid the effects of external disturbances, output signals from the force sensor and the NN are filtered by the Butterworth filter, where the cut-off frequencies are set at 25 and 3 Hz, respectively.

2) Experimental Results: Fig. 16 shows an example of experimental results with the assist ratio $\alpha = 1$. Each panel shows, in order from the top, a time history of the desired signal r, the control signal y, the assisted signal y_s, the control error e, the hand force f, the assisting signal Δ_y, and the identification error ϵ. The tracking control performance improved remarkably by adding assistance from the robotic system, but it was difficult for a novice operator to track the given desired signal well.
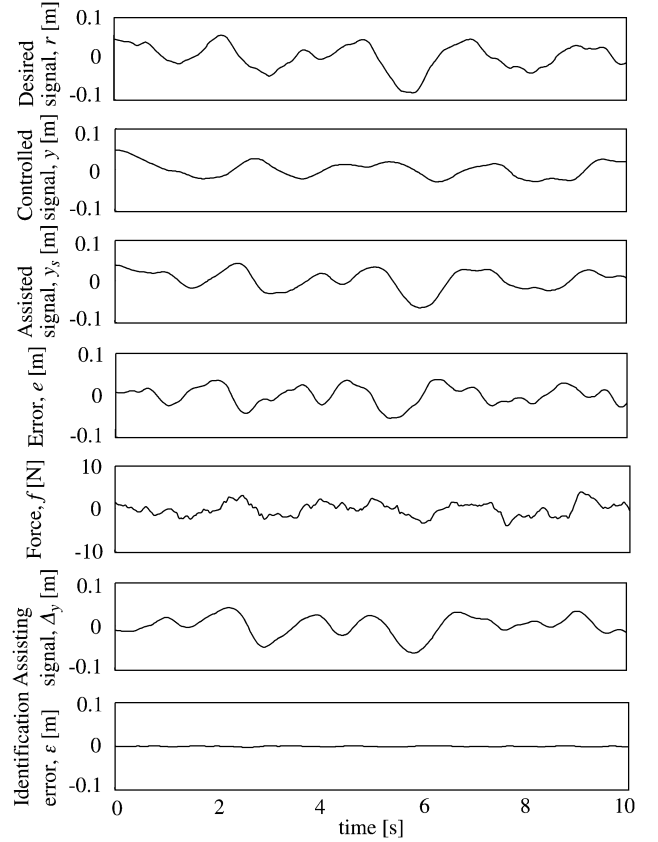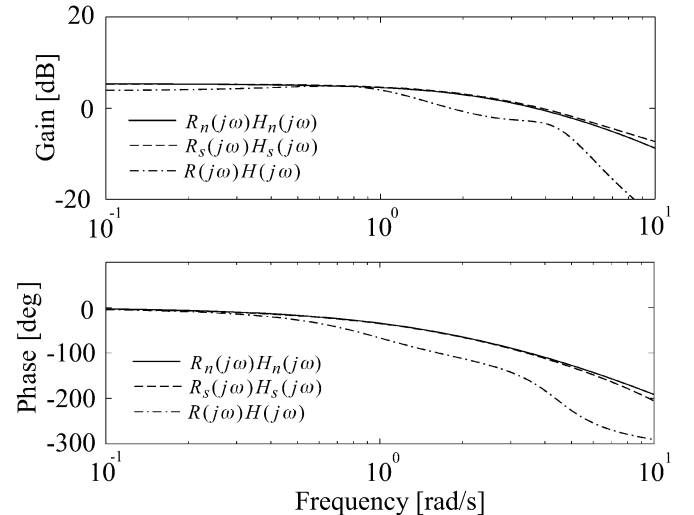
Fig. 17.   Describing functions estimated from experimental results under the proposed method.

Fig. 17 shows estimated describing functions with experimental results. In this figure, the solid line shows the reference model $R_n(j\omega)H_n(j\omega)$, the dotted line shows the estimated overall system characteristics with the assisting signal $R_s(j\omega)H_s(j\omega)$, and the dashed line shows without the assisting signal $R(j\omega)H(j\omega)$. The gain characteristics of $R(j\omega)H(j\omega)$ is considerably lower in the high frequency range than the one of the reference model; there also exists a serious phase lag in $R(j\omega)H(j\omega)$. However, by giving assistance, the
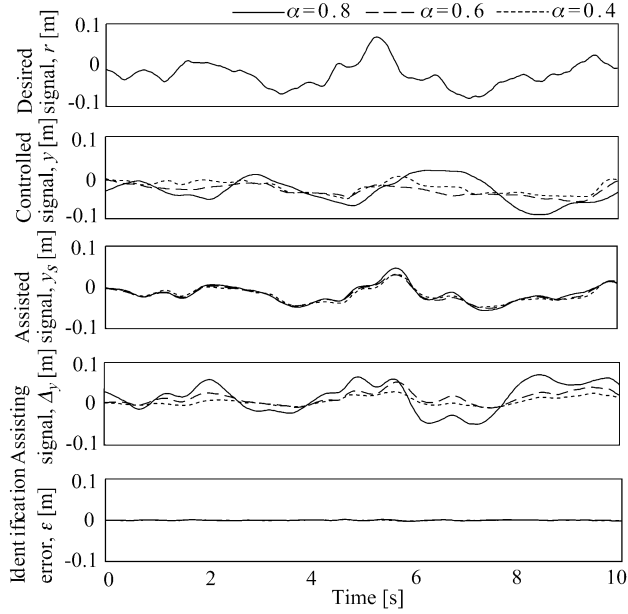
Fig. 18. Changes of the control results depending on the assisting ratio α.

gain characteristics improved in the high frequency range and the phase lag is compensated, as shown in $R_s(j\omega)H_s(j\omega)$. Consequently, the overall system characteristics with robotic assistance almost agree with those of the reference model. We confirmed the basic behavior of the proposed training system.

In the proposed training system, the level of robotic assistance can be adjusted by changing the assist ratio α. For instance, when $\alpha = 1$, the target control characteristics specified by the reference model is always realized without depending on the human control action, as long as identification by the NN is carried out with good accuracy. Therefore, this system is suitable for showing a good control example to a trainee because the robot moves the trainee's hand following the predicted hand trajectory of the skillful human operator. In contrast, using a small value of α, a trainee must track the desired trajectory with a small amount of robotic assistance. Experiments were conducted using different assist ratios ($\alpha = 0.8, 0.6, 0.4$) to investigate the influence of α on human movements during training. Each subject was asked to perform the tracking test in the order of $\alpha = 0.8, 0.6, 0.4$. The number of trials was three for each assist ratio α, with brief intervals when α was changed.

Fig. 18 shows examples of experimental results. The figure shows, from the top, the time history of the desired signal r, the controlled signal y, the assisted signal y_s, the assisting signal Δ_y, and the identification error ϵ. In the figure, the solid line shows the case of $\alpha = 0.8$, the dashed line $\alpha = 0.6$, and a dotted line $\alpha = 0.4$. As the assist ratio decreases, the assisting signal Δ_y does also. However, it is interesting that the assisted signals y_s are almost identical for all α. This similarity illustrates the training effect.

In addition to the two indexes J and U_x given in (2) and (3), an index on the tracking control performance without robotic assistance is defined as

$$J_\alpha = \frac{\int_0^{t_f} \left(r(t) - y(t) \right)^2 dt}{\int_0^{t_f} r^2(t) dt}. \tag{21}$$
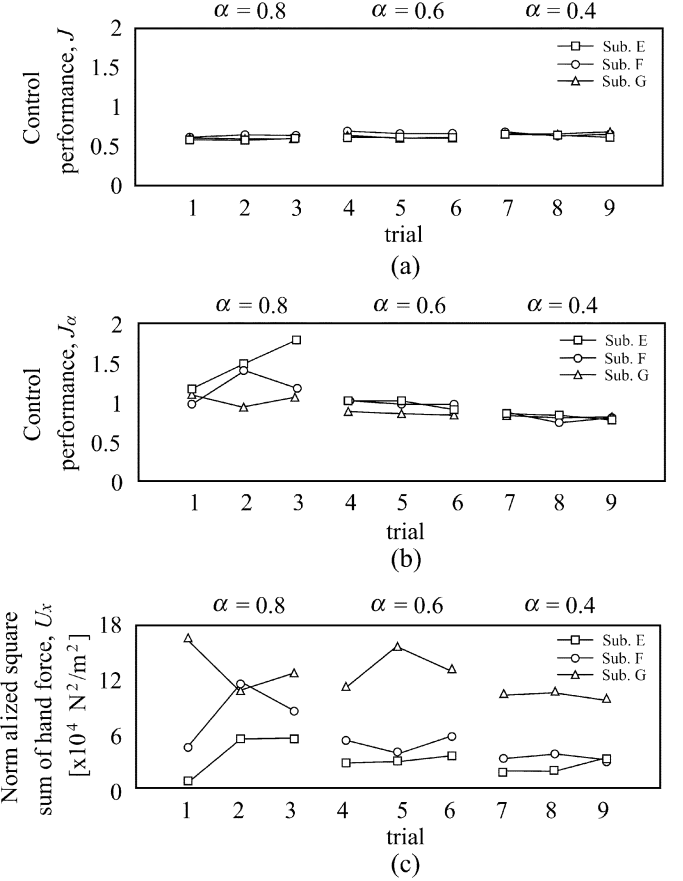
Fig. 19. Changes of the control performances J, J_α and the normalized square sum of hand force U_x depending on the number of trials for all subjects.
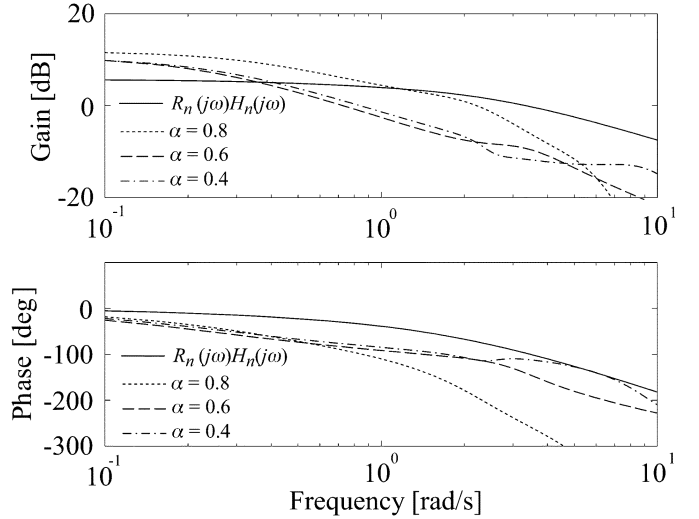
Fig. 20. Changes of the estimated describing functions depending on the assisting ratio α.

The difference between J and J_α is caused by assistance. Fig. 19 shows changes of the performance indexes J, J_α, and U_x for all subjects according to the assist ratio α with respect to the number of trials when the operation time per trial is $t_f = 60$ [s]. The tracking control ability was trained when $\alpha = 0.4, 0.6$, since the control performance J_α was improved during trials in spite of the reduced assistance. On the other

hand, the results showed that the training under $\alpha = 0.8$ is not effective because both J_α and U_x increase. However, for all α, the tracking control performance, J, is maintained at around 0.6. Therefore, the overall system is always stable.

Finally, Fig. 20 presents describing functions of the overall system $\hat{R}(j\omega)\hat{H}(j\omega)$ estimated from experimental results. In this figure, a solid line shows the characteristics of the reference model, a dotted line shows the case with $\alpha = 0.8$ in the third trials, a broken line shows $\alpha = 0.6$, and an alternate long and short dash line shows $\alpha = 0.4$. In comparison with the results when $\alpha = 0.6$ and 0.4, the phase lag of increases when $\alpha = 0.8$. In other words, even if a human operator achieves a large gain, the control performance J_α worsens because of the large phase lag. These facts show that the operator changes the control property according to the degree of the assistance. Consequently, it can be seen that a desirable value of the assist ratio α is less than 0.6. Adaptive adjustment of α according to the control performance of a trainee may improve the effectiveness of the proposed method.

VI. CONCLUSION

This paper has analyzed changes of the tracking control properties of a human–robotic system according to the robot impedance, the proficiency of operators, and the impedance property of the human arm. Thereby, the following characteristics are obtained.

1) The human control property depends considerably on the robot impedance.
2) The control property of a human–robotic system is almost invariable within some range of robot impedance.
3) The control performance of the overall system decreases slightly when the robot becomes unstable or the operator must generate a large operational force.
4) The variability of human arm impedance fulfills an important role.

Then, the design method of a training system using the NN for operating power-assist systems has been discussed using experimental results obtained in the manual tracking control task. The proposed training system can identify human characteristics with the reference model of a human–robotic system through on-line learning of the NN. Simultaneously, it assists a trainee to improve the tracking control performance based on the identification results. Preliminary training experiments were conducted with the unskilled subjects to verify basic behaviors of the proposed adaptive training system with respect to the assist ratio. The results demonstrate that the proposed method can attain the desired control property of a human–robotic system by the reference model with a modeling error, and that the operational load of a trainee can be changed by regulating α. Although effectiveness of the proposed training system should be further examined, the design method has the potential for developing a rehabilitation system using a robot for a physically handicapped person who uses prosthesis or an orthosis.

Future research will be directed to investigate the control performance with the change of motion direction, the influence of normal hand force f_y on performing tasks, and the control properties with other target signals such as a cyclic signal and a random signal with high frequency components. In addition, we plan to develop a design method of the reference model for specific tasks and an algorithm of adaptive regulation of the assist ratio α according to the level of trainee's skill. We also plan to extend the proposed methodology available for actual human–robotic systems with multiple degrees of freedom, considering with the dependence of human control properties on the arm configuration and the operational direction.

REFERENCES

[1] W. A. Gruver, "Intelligent robotics in manufacturing, service, and rehabilitation: An overview," *IEEE Trans. Ind. Electron.*, vol. 41, pp. 4–11, Feb. 1994.
[2] M. Hans, B. Graf, and R. D. Schraft, "Robotic home assistant care-o-bot: Past-present-future," in *Proc. ROMAN*, 2001, pp. 407–411.
[3] Y. Yamada, T. Morizone, Y. Umetani, and H. Konosu, "Warning: To err is human," *IEEE Robot. Autom. Mag.*, vol. 11, no. 2, pp. 34–45, Jun. 2004.
[4] H. Kazerooni, "Human–robot interaction via the transfer of power and information signals," *IEEE Trans. Syst., Man, Cybern.*, vol. 20, pp. 450–463, Mar./Apr. 1990.
[5] Y. Yokokohji, "The theory of master-slave control" (in Japanese), *J. Robot. Soc. Jpn.*, vol. 11, no. 6, pp. 794–802, 1993.
[6] Y. Yokokohji and T. Yoshikawa, "Bilateral control of master-slave manipulations for ideal kinesthetic coupling," in *Proc. IEEE Int. Conf. Robot. Autom.*, 1992, pp. 849–858.
[7] J. E. Colgate, "Robust impedance shaping telemanipulation," *IEEE Trans. Robot. Autom.*, vol. 9, pp. 374–384, Aug. 1993.
[8] K. Kosuge, Y. Fujisawa, and T. Fukuda, "Control of mechanical system with man-machine interaction," in *Proc. IEEE Int. Conf. Intell. Robots Syst.*, 1992, pp. 87–92.
[9] K. Kosuge and N. Kazamura, "Control of a robot handling an object in cooperation with a human," in *Proc. IEEE Int. Workshop Robot Human Commun.*, 1997, pp. 142–147.
[10] O. M. Al-Jarrah and Y. F. Zheng, "Arm-manipulator coordination for load sharing using compliant control," in *Proc. IEEE Int. Conf. Robot. Autom.*, 1996, pp. 1000–1005.
[11] ——, "Arm-manipulator coordination for load sharing using reflexive motion control," in *Proc. IEEE Int. Conf. Robot. Autom.*, 1997, pp. 2326–2331.
[12] R. Ikeura, "Manual control approach to the teaching of a robot task," *IEEE Trans. Syst., Man, Cybern.*, vol. 24, pp. 1339–1346, Sep. 1994.
[13] R. Ikeura and H. Inooka, "Variable impedance control of a robot for cooperation with a human," in *Proc. IEEE Int. Conf. Robot. Autom.*, 1995, pp. 3097–3102.
[14] T. Tsumugiwa, R. Yokogawa, and K. Hara, "Variable impedance control based on estimation of human arm stiffness for human–robot cooperative calligraphic task," in *Proc. IEEE Int. Conf. Robot. Autom.*, 2002, pp. 644–650.
[15] F. A. Mussa-Ivaldi, N. Hogan, and E. Bizzi, "Neural, mechanical and geometrical factors sub-serving arm posture in humans," *J. Neurosci.*, vol. 5, no. 10, pp. 2732–2743, 1985.
[16] T. Tsuji, P. G. Morasso, K. Goto, and K. Ito, "Human hand impedance characteristics during maintained posture," *Biol. Cybern.*, vol. 72, pp. 475–485, 1995.
[17] T. Tsuji, M. Moritani, M. Kaneko, and K. Ito, "An analysis of human hand impedance characteristics during isometric muscle contractions" (in Japanese), *Trans. Soc. Instrum. Control Eng.*, vol. 32, no. 2, pp. 271–280, 1996.
[18] T. Tsuji, "Human arm impedance multijoint movements, self-organization," in *Computational Maps, and Motor Control*, P. Morasso, Ed. New York: Elsevier , 1997, pp. 357–381.
[19] H. Gomi and R. Osu, "Task-dependent viscoelasticity of human multijoint arm and its spatial characteristics for interaction with environments," *J. Neurosci.*, vol. 18, no. 21, pp. 8965–8978, 1998.
[20] N. Hogan, "Controlling impedance at the man/machine interface," in *Proc. IEEE Int. Conf. Robot. Autom.*, 1989, pp. 1626–1629.
[21] O. Fukuda, T. Tsuji, A. Ohtsuka, and M. Kaneko, "EMG-based human–robot interface for rehabilitation aid," in *Proc. IEEE Int. Conf. Robot. Autom.*, 1998, pp. 3492–3497.

[22] K. F. Kraiss, "Implementation of user-adaptive assistants with neural operator models," *Control Eng. Prac.*, vol. 3, no. 2, pp. 249–256, 1995.

[23] K. KrishnaKumar, S. Sawhney, and R. Wai, "Neuro-controllers for adaptive helicopter hover training," *IEEE Trans. Syst., Man, Cybern.*, vol. 24, no. 8, pp. 1142–1152, Aug. 1994.

[24] O. Suenaga, "A study on computing method of predicted value of controlled variable on manual preview-predictive control systems" (in Japanese), *Jpn. J. Ergon.*, vol. 31, no. 6, pp. 407–414, 1995.

[25] K. J.Åström and B. Wittenmark, *Adaptive Control*.   Reading, MA: Addison-Wesley, 1989.

[26] N. Hogan, "Impedance control: An approach to manipulation, parts I, II, III," *Trans. ASME, J. Dynamic Syst., Measure., Control*, vol. 107, no. 1, pp. 1–24, 1985.

[27] ——, "Stable execution of contact tasks using impedance control," in *Proc. IEEE Int. Conf. Robot. Autom.*, 1987, pp. 1047–1054.

[28] P. V. Overschee and B. D. Moor, "N4SID: Subspace algorithms for the identification of combined deterministic-stochastic system," *Automatica*, vol. 30, no. 1, pp. 75–93, 1994.

[29] D. T. McRuer and H. R. Jex, "A review of quasi-linear pilot models," *IEEE Trans. Human Factors Electron.*, vol. 5, no. 8, pp. 231–249, Aug. 1967.

[30] H. Konosu, Y. Yamada, T. Morizono, and Y. Umetani, "Study on the control strategy for a human power assisting system with task condition variations" (in Japanese), in *Proc. 16th Annu. Meeting Robot. Soc. Jpn.*, 1998, pp. 947–948.

[31] A. Sano, H. Fujimoto, and K. Matsushita, "Skill transfer by coaching (skill-up process and weak point)" (in Japanese), in *Proc. 4th Robot. Symp.*, 1999, pp. 307–312.

[32] T. Tsuji, B. H. Xu, and M. Kaneko, "Adaptive control and identification using one neural network for a class of plants with uncertainties," *IEEE Trans. Syst., Man, Cybern. A, Syst. Humans*, vol. 28, no. 4, pp. 496–505, Jul. 1998.

[33] J. L. Elman, "Finding structure in time," *Cogn. Sci.*, vol. 14, pp. 179–211, 1990.

[34] D. E. Rumelhart and J. L. McClelland, *Parallel Distributed Processing, Explorations in the Microstructure of Cognition*.   Cambridge, MA: MIT Press, 1986, vol. 1, ch. 8, pp. 318–362.

Toshio Tsuji (A'88–M'99) received the B.E. degree in industrial engineering his M.E. and Doctor of Engineering degrees in systems engineering from Hiroshima University, Hiroshima, Japan, in 1982, 1985, and 1989, respectively.

He was a Research Associate from 1985 to 1994, and an Associate Professor, from 1994 to 2002, with the Faculty of Engineering, Hiroshima University. He was a Visiting Professor at the University of Genova, Genova, Italy for one year from 1992 to 1993. He is currently a Professor of Department of Artificial Complex Systems Engineering, Hiroshima University. His current research interests have focused on human–machine interface and computational neural sciences, in particular, biological motor control.

Dr. Tsuji is a Member of the Japan Society of Mechanical Engineers, the Robotics Society of Japan, and the Society of Instrumentation and Control Engineers in Japan. He won the Best Paper Award from The Society of Instrumentation and Control Engineers in 2002 and the K. S. Fu Memorial Best Transactions Paper Award of the IEEE Robotics and Automation Society in 2003.

Yoshiyuki Tanaka (M'04) received the B.E. degree in computer science and systems engineering from Yamaguchi University, Japan, in 1995 and the M.E. and Dr. of Engineering degrees in information engineering from Hiroshima University, Hiroshima, Japan, in 1997 and 2001, respectively.

From 2001 to 2002, he was a Research Associate with the Faculty of Information Sciences, Hiroshima City University. He is currently a Research Associate in the Department of Artificial Complex Systems Engineering, Hiroshima University, Hiroshima, Japan. His research interests include biological motor control and human–machine interaction.

Dr. Tanaka is a Member of the Robotics Society of Japan, the Institute of Electrical Engineering of Japan, and the Society of Instrumentation and Control Engineers in Japan.